https://doi.org/10.5194/egusphere-2026-5280
Preprint. Discussion started: 16 November 2026
© Author(s) 2026. CC BY 4.0 License.

Validation of diffusive samplers for the simultaneous measurement of nitrogen oxides

Valerio Ferracci[1], Benjamin Michen[2], Erin Cackett[1], Yassine Wakim[1], Yaser Showman[1], Thomas G. Holmes[1], Linda S. Gates[3], David C. Green[4], Anja H. Tremper[4], Nicholas A Martin[1]

[1]Air Quality and Aerosol Metrology, National Physical Laboratory, Teddington, TW11 0LW, United Kingdom
[2]Passam AG, Schellenstrasse 44, 8708, Männedorf, Switzerland
[3]Gradko International Ltd, 77 Wales St, Winchester, SO23 0RH, United Kingdom
[4]Environmental Research Group, Imperial College London, 86 Wood Lane, London, W12 0BZ, United Kingdom

Correspondence to: Valerio Ferracci (valerio.ferracci@npl.co.uk)

Abstract. Poor air quality is a major threat to human and ecosystem health, and policies aimed at abating air pollution rely on ambient monitoring to apportion sources, validate inventories and assess the efficacy of interventions. Nitrogen oxides (NO_x ≡ NO + NO_2) are key air quality pollutants and their monitoring relies on complex and resource-intensive reference instrumentation. Diffusive samplers offer a cost-effective way to monitor NO_x across entire localities, overcoming some of the limitations of reference instruments. This study determined the diffusive sampling rates of three types of commercially available samplers (Passam AG's NO_2 and NO_x samplers, Gradko International's NO_2 samplers) and one currently under development (Gradko's NO_x samplers). Samplers were exposed monthly at an air quality monitoring station in central London from November 2022 to February 2025. In addition, laboratory exposures of the same sampler types were performed in the Controlled Atmosphere Test Facility (CATFAC). During all exposures, samplers were co-located with reference analysers providing traceable NO_x concentrations. After exposure the samplers were returned to the respective manufacturers for chemical analysis, and the reported nitrite results were combined with the reference data and exposure times to determine the experimental NO and NO_2 diffusive sampling rates, U_{NO} and U_{NO_2} respectively. Measured diffusive sampling rates at standard conditions (T = 20 °C and p = 101.3 kPa) for the Passam samplers were U_{NO} = (5.67 ± 0.20) × 10^{-5} m^3 h^{-1} and U_{NO_2} = (4.73 ± 0.11) × 10^{-5} m^3 h^{-1}. The sampling rate for the new design of the Gradko NO_2 sampler (prepared with a 50 % TEA/acetone coating) was U_{NO_2} = (6.80 ± 0.14) × 10^{-5} m^3 h^{-1}, consistent with that from an earlier design (with 20 % TEA/H_2O coating) and indicating that different sorbent recipe had no measurable effect on U_{NO_2}. U_{NO} for the Gradko samplers was U_{NO} = (1.92 ± 0.20) × 10^{-5} m^3 h^{-1}, below the value expected from molecular diffusivities. Further tests indicated that the oxidant formulation in the Gradko NO_x samplers required further optimisation to achieve quantitative conversion of NO to NO_2 throughout the exposure period. Storage tests were carried out to establish the effects of time on the extracted nitrite, and indicated good stability of the adsorbed nitrite over timescales of 2-3 months. Analysis of environmental influences showed no significant temperature dependence after normalisation to standard conditions, while evidence was found for minor effects associated with ozone concentrations and high analyte loadings. This work provides traceable validation of diffusive samplers

https://doi.org/10.5194/egusphere-2026-5280
Preprint. Discussion started: 16 November 2026
© Author(s) 2026. CC BY 4.0 License.

for the simultaneous measurement of NO and NO_2 and demonstrates their potential to deliver spatially resolved NO_x data for air quality assessment, emissions inventory verification and atmospheric model evaluation.

1 Introduction

Poor air quality is a major threat to human health, with the combined effects of ambient and indoor air pollution contributing to an estimated 6.7 million premature deaths a year *via* increases in chronic conditions such as cardiovascular and respiratory diseases, all of which reduce life expectancy (World Health Organization, 2015). The European Union and the UK have implemented clean air policies and set standards to limit the emissions of key pollutants through the Air Quality Directives (EU Directive 2008/50/EC, 2008; EU Directive 2024/2881, 2024), and other closely aligned legislation (UK Environment Act 2021, 2021). These include measures to reduce levels of nitrogen dioxide (NO_2), which is a key precursor to the formation of ozone (O_3) and fine particulate matter, two other regulated air pollutants that significantly impact public health. Most anthropogenic NO_2 originates from emissions of nitric oxide (NO) from combustion sources *e.g.*, road transport (Vestreng et al., 2009), and space and water heating (Cliff et al., 2025). NO is subsequently converted into NO_2 by reaction with O_3. NO_2 can be converted back to NO *via* a variety of processes, including direct photolysis and further chemical reactions. Due to their rapid interconversion, NO and NO_2 are in steady state and are referred to collectively as total nitrogen oxides (NO_x). The simultaneous measurement of NO and NO_2, *i.e.* NO_x, is key to understanding air quality and to validating emission inventories and atmospheric models.

A number of techniques are used to measure nitrogen oxides. Online methods include chemiluminescence (Alam et al., 2020), which is also the reference method in the UK and EU (BS EN 14211:2024, 2024), cavity attenuated phase shift spectroscopy or CAPS (Kebabian et al., 2008), long path absorption photometry or LOPAP for NO_2 (Villena et al., 2012). Most online methods are resource intensive, requiring dedicated temperature-controlled enclosures with mains power supply along with specialist regular maintenance and calibration, limiting the number of monitoring sites available. While small sensor systems for air quality have emerged over the last decade (Mead et al., 2013; Popoola et al., 2018), these are still undergoing evaluation and standardisation to address their many drawbacks and ensure they are suitable for air quality monitoring (Diez et al., 2025; Hayward et al., 2024).

Within this context, diffusive samplers offer many practical advantages for ambient air monitoring: they are low-cost and easy to deploy, so they can cover large geographical areas, allowing to capture the granularity of air pollution. Diffusive samplers for NO_2 were first developed for occupational exposure (Palmes et al., 1976) and consist of an acrylic tube with a capped end at the top and an open end at the bottom. A stainless-steel grid, coated in a sorbent compound (typically triethanolamine, or TEA), is placed at the capped end of the sampler. Ambient air diffuses from the open end and, once it reaches the TEA-coated grid, any NO_2 present reacts to form nitrite (NO_2^-), which is irreversibly trapped on the grid. Following exposure, the mass of

https://doi.org/10.5194/egusphere-2026-5280
Preprint. Discussion started: 16 November 2026
© Author(s) 2026. CC BY 4.0 License.

the collected nitrite is determined by spectrophotometry in the laboratory (see Section 2.4). If the diffusive sampling rate of NO_2 is known, the mass of nitrite collected can be used to determine the average concentration of NO_2 in the sampled air over the exposure period (Brown et al., 2025).

Diffusion samplers are widely employed in many localities to monitor NO_2; however they suffer from well-known environmental biases *e.g.*, from temperature, relative humidity and other pollutants (Heal et al., 2019). They can also be adversely affected by wind: high wind speeds can cause turbulence at the open end of the samplers, shortening the diffusive pathlength and increasing the effective sampling rate (Cape, 2009; Martin et al., 2014). In the UK, biases in NO_2 measurements by diffusive samplers are corrected by the application of annually determined bias adjustment factors (Department for Environment, Food & Rural Affairs, 2025b), an approach that has been demonstrated to meet the requirements of indicative measurements (EU Directive 2008/50/EC, 2008), *i.e.* with an expanded uncertainty ≤ 25 % for the annual average NO_2 concentration (Butterfield et al., 2021). Alternatively, shelters or wind protection caps have been shown to alleviate the biases introduced by wind turbulence (Hafkenscheid et al., 2009; Martin et al., 2014; Medland et al., 2025). These modification improve the measurement quality of NO_2 diffusion samplers significantly, achieving the requirements for fixed measurements for the annual average NO_2 concentration (an expanded uncertainty ≤ 15 %), without the need for bias adjustment (Butterfield et al., 2021).

Recent efforts in the UK have focused on deploying wind-capped NO_2 diffusive samplers in target areas where air quality models indicate an exceedance of the annual mean limit value of 40 µg m^{-3}, and where there are differences in the NO_2 concentrations predicted by the Department for Environment, Food & Rural Affairs' Pollution Climate Mapping (PCM) model and those determined by other local models (Department for Environment, Food & Rural Affairs, 2025d). As NO_2 originates from the rapid reaction of NO with O_3, simultaneous measurements of NO and NO_2 would deliver valuable data on NO_x emissions to improve and validate air quality models. This is currently not possible to achieve inexpensively due to prohibitive costs and practical limitations involved in deploying additional NO_x reference instruments. Diffusion samplers measuring total NO_x are available: these are based on the design of NO_2 samplers and incorporate an oxidant facilitating the conversion of NO into NO_2, which is then trapped as nitrite on the sorbent. Some designs incorporate an oxidant consisting of granular aluminium coated with potassium chromate and chromium V, located above the TEA-coated grid at the capped end of the sampler (Vardoulakis et al., 2009). In other types of NO_x samplers (including the two products tested in this work) the oxidant is incorporated in the coating of the stainless-steel mesh along with the TEA sorbent. Regardless of the specific design of the sampler, the additional NO_2 generated from the oxidation of NO is also trapped on the TEA as nitrite: therefore, in the case of NO_x samplers, the total collected nitrite is a measure of the sum of NO and NO_2 *i.e.*, NO_x. The average concentration of NO during the exposure period can then be calculated as the difference between co-located pairs of NO_x and NO_2 samplers, provided the NO and NO_2 diffusive sampling rates, U_{NO} and U_{NO_2}, are known. While available for many decades (Laitinen et al., 1993; Sánchez Jiménez et al., 2011; Vardoulakis et al., 2009), NO_x diffusive samplers have undergone comparatively less

https://doi.org/10.5194/egusphere-2026-5280
Preprint. Discussion started: 16 November 2026
© Author(s) 2026. CC BY 4.0 License.

validation than their NO_2 counterparts, potentially due to air quality regulations focusing primarily on NO_2. This in turn limits their uptake for air quality monitoring.

In this work we describe the validation of two types of diffusive samplers for the simultaneous measurement of NO and NO_2. The experimental NO and NO_2 diffusive sampling rates, U_{NO} and U_{NO_2} , for both sets of samplers were determined by laboratory and field studies. Results from storage tests, to ascertain the stability of the samplers after exposure, and those from oxidant tests, to establish the effects of varying oxidant abundances for one of the suppliers, are also presented.

2 Methods

2.1 Diffusive samplers

Two designs of diffusive samplers were evaluated in the current study, one from Gradko International and one from Passam AG. Each set consisted of pairs of NO_2 and NO_x samplers. The NO_2 and NO_x samplers from Passam and the NO_2 samplers from Gradko are commercially available, while the Gradko NO_x samplers are currently under development.

The Gradko samplers consisted of sets of two diffusion tubes, one for NO_2 and one for total NO_x. The stainless-steel grid at the capped end of the Gradko NO_x samplers was coated in TEA and a chemical oxidant (2-Phenyl-4,4,5,5-tetramethylimidazoline-1-oxyl 3-oxide, or PTIO). The sorbent recipe for both NO_2 and NO_x samplers was changed from the original design of 20 % TEA in water to 50 % TEA in acetone, as the PTIO is more soluble in the latter. The Gradko diffusive samplers were equipped with an amorphous polyethylene filter at the open end to reduce measurement biases due to wind turbulence (Martin et al., 2014). The samplers were delivered to NPL with the wind protective filter already fitted in a sealable vial housed in an outer resealable plastic bag. The samplers were removed from their vials for exposure. After exposure, the protective filters were removed and replaced with endcaps for transportation. Figure 1a shows a photograph of the Gradko NO_2 and NO_x samplers.

The Passam samplers also consisted of sets of two diffusive samplers with protective wind filters, one with and one without oxidant. In this case, details such as the nature of the oxidant are proprietary and were not stated in the technical datasheet (Passam AG, 2020). The Passam samplers arrived at NPL with endcaps fitted. These were removed and replaced with wind protective filters. After exposure, the filters were removed and replaced with the original endcaps for transportation. Figure 1b shows a photograph of the Passam NO_2 and NO_x samplers.

For each deployment (whether in the laboratory or in the field) both Gradko and Passam provided six sets of NO_2/NO_x sampler pairs. One set of samplers from each manufacturer remained capped and acted as the travel blank. All samplers were

https://doi.org/10.5194/egusphere-2026-5280
Preprint. Discussion started: 16 November 2026
© Author(s) 2026. CC BY 4.0 License.

transported in a resealable bag and, whilst in storage at NPL, were kept refrigerated at a temperature of 4 °C within a resealable plastic bag until required for deployment or despatch to the manufacturer for analysis.

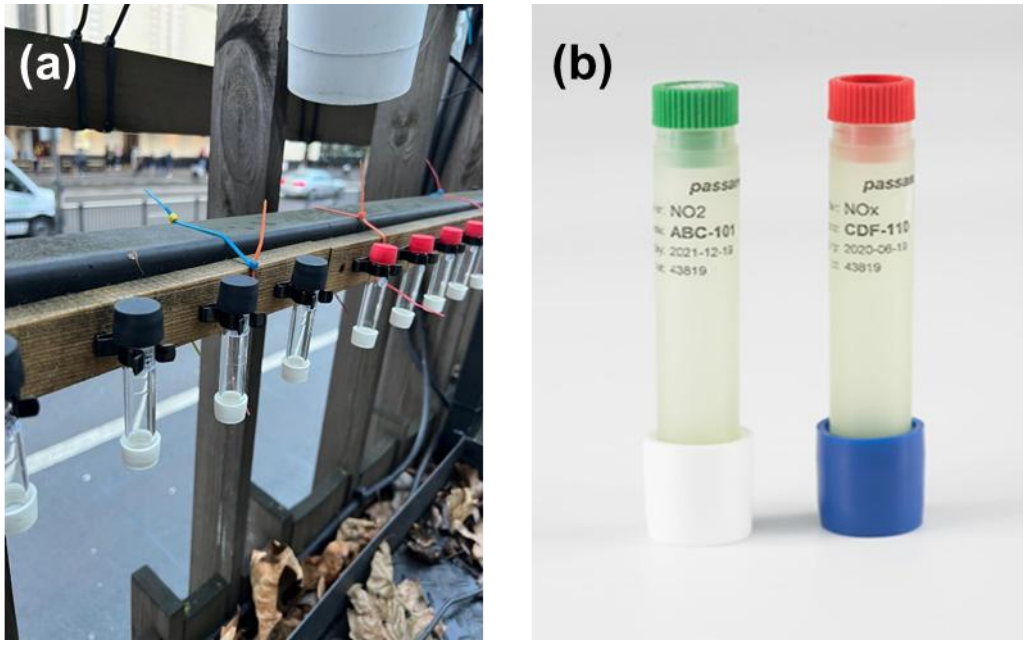


Figure 1: Photographs showing a) Gradko and b) Passam NO_2 and NO_x samplers.

2.2 Field exposures

Sets of NO_2/NO_x diffusive samplers from Gradko and Passam were deployed each month between November 2022 and February 2025 at the air quality monitoring supersite at Marylebone Road, an urban traffic site in central London (51.522530°N, 0.154611°W). The site is located in a typical street canyon on the side of a busy six-lane road, often congested.

All samplers were installed on the roof of the monitoring station (Figure 2). Gradko samplers were mounted in specialised tube holders, while those from Passam were mounted in separate protective shelters. The exposure time was either four or five weeks, and was aligned with the requirements of the UK national calendar for local air quality monitoring (Department for Environment, Food & Rural Affairs, 2025c).

The samplers were co-located with a reference analyser (Teledyne API 200E), which delivered the NO_2 and NO reference measurements. Ratified hourly reference data were downloaded from the Automatic Urban and Rural Network (AURN) website (Department for Environment, Food & Rural Affairs, 2025a). These were then used to calculate the mean NO_2 and

https://doi.org/10.5194/egusphere-2026-5280
Preprint. Discussion started: 16 November 2026
© Author(s) 2026. CC BY 4.0 License.

NO concentrations during the exposure periods. The reference NO and NO_2 mean concentrations, along with data capture, mean ozone concentrations, temperature and wind speed (all used for further analysis, see Section 4.2) are shown in Table 1. Only exposures where the data capture was > 85 % were used for the analysis of diffusion tube data.



Figure 2: Field deployment of Gradko and Passam NO_x samplers at Marylebone Road, central London. Gradko samplers are mounted on dedicated brackets, while Passam samplers are housed in cylindrical protective shelters.

2.3 Laboratory exposures

Sets of NO_2 and NO_x diffusive samplers from Gradko and Passam were also deployed inside the Controlled Atmosphere Test Facility (CATFAC) at the National Physical Laboratory (NPL), the UK's National Metrology Institute. It consists of a custom-built temperature-controlled wind tunnel with an internal volume of approximately 1000 L. It simulates exposure of diffusive samplers to atmospheres of accurate composition under controlled environmental conditions (temperature, relative humidity and wind speed). The test atmosphere is introduced in a section of the CATFAC with turbulent flow, to ensure good mixing. A stainless-steel recirculating blower (Eurotherm Drives) drives the gas mixture through a series of restricting grids designed

https://doi.org/10.5194/egusphere-2026-5280
Preprint. Discussion started: 16 November 2026
© Author(s) 2026. CC BY 4.0 License.

to ensure a uniform, laminar airflow in the section of the facility where the diffusive samplers are deployed. This minimises the effects of air turbulence and ensures the uptake of analyte by the samplers is driven primarily by diffusion. Diffusive samplers measuring volatile organic compounds (Martin et al., 2003, 2005), NO_2 (Martin et al., 2014) and ammonia (Martin et al., 2019) were previously tested and validated using the CATFAC.

In this study, several multiple-component atmospheres were generated containing NO_2 and NO at traceable concentrations of relevance to air quality monitoring applications. Each exposure period in the laboratory was four weeks. The required NO_2 and NO gas concentrations were achieved by dynamically blending and diluting certified gas mixtures (BOC, 26.7 ± 0.5 µmol mol^{-1} NO_2 in N_2 and 101 ± 1 µmol mol^{-1} NO in N_2) with scrubbed air (Peak Scientific) using an array of calibrated mass flow controllers (Brooks Instruments).

The test atmospheres were continuously replenished in the CATFAC at a rate of approximately 30 L min^{-1} with a freshly generated mixture of the same concentration. The blower was calibrated using a traceable anemometer (Testo 416, 16 mm Vane Anemometer) in the sampler deployment section, indicating a wind speed within the facility of 1.4 ± 0.2 m s^{-1}, which is within the range of previous diffusive sampler studies (Martin et al., 2014, 2019). The diffusive samplers were distributed in the exposure section of the chamber perpendicular to the direction of gas flow (Figure 3).



Figure 3: Deployment configuration of NO_2 and NO_x samplers inside the Controlled Atmosphere Test Facility (CATFAC)

A calibrated chemiluminescence reference analyser (Thermo Scientific, 42i) sampled from the test chamber and was calibrated bi-weekly with a traceable gas mixture (BOC, 454 ± 13 nmol mol^{-1} of NO_x in N_2, of which 453 nmol mol^{-1} of NO in N_2).

The chamber temperature was maintained at the target value of 20 ± 1 °C using a chiller/heater control system (Grant Instruments) pumping a mixture of ethylene glycol and water through copper coils wrapped around the CATFAC. The facility

https://doi.org/10.5194/egusphere-2026-5280
Preprint. Discussion started: 16 November 2026
© Author(s) 2026. CC BY 4.0 License.

was further wrapped in glass fibre insulation to prevent "cold spots" and any potential water condensation on the inside walls. The required relative humidity, nominally 70 %, was delivered by a water vapor generation unit (IGI Systems Ltd): a known flow rate of pure de-ionised liquid water (Elga DV 35 Purelab), calibrated by gravimetry, was passed through a vaporiser; the resulting water vapour was swept by a controlled flow of zero air, which then mixed with the main gas flow containing NO and NO_2. Temperature and humidity inside the CATFAC were independently monitored by calibrated probes.

2.4 Analysis of diffusive samplers

In all samplers, NO_2 (either from ambient air or from the oxidation of NO at the coated grid) reacted with the sorbent TEA and was converted into nitrite (NO_2^-). Exposed samplers were then analysed by the manufacturers using colorimetry (BS EN 16339:2025, 2025). This is a well-established method, and therefore only a brief description is provided here. A purple azo dye consisting of a solution of naphthyl-1-ethylene diamine dihydrochloride (NEDD), sulphanilamide, and orthophosphoric acid, is added to the diffusion tube. The nitrite dissolves in the dye and the absorbance of the resulting solution at λ = 540 nm is then measured with a UV-visible spectrophotometer calibrated with standard nitrite solutions. Absorbance is then converted into mass of nitrite using Beer-Lambert's Law.

2.5 Storage tests

To establish whether exposed diffusive samplers degraded with time, a series of storage tests were carried out. For samplers from Gradko, this involved deploying two additional batches (each consisting of five NO_2 and five NO_x samplers) at Marylebone Road in July 2023. After exposure, one batch was treated as normal and returned to Gradko for immediate analysis; the other two batches were retained and stored in a refrigerator at 4 °C. The second and third batches were dispatched for analysis after two and three months, respectively.

For Passam samplers, a different approach was taken due to logistics. Initially, two batches (each consisting of five NO_2 and five NO_x samplers) were deployed in the field in July 2023. After exposure, one batch was treated as normal and returned to Passam for immediate analysis; the other batch was retained and stored in a refrigerator at 4 °C for two months before being despatched for analysis. A similar procedure was repeated in August 2023, with the stored batch retained for three months before being sent to Passam for analysis.

2.6 Oxidant tests

Following a preliminary analysis, the NO sampling rate for the Gradko samplers was significantly lower than expected from the diffusivity of NO relative to that of NO_2 (see Section 3.2 below for details). Tests were carried out to ensure that there was sufficient PTIO oxidant in the Gradko NO_x samplers to convert all the ambient NO into NO_2. These entailed deploying the standard Gradko NO_x samplers along with additional sets containing an increased amount of PTIO: if sufficient oxidant was present in all samplers, any NO in ambient air would be efficiently converted to NO_2 so that there should be no difference,

https://doi.org/10.5194/egusphere-2026-5280
Preprint. Discussion started: 16 November 2026
© Author(s) 2026. CC BY 4.0 License.

within the experimental uncertainty, between a standard batch and one with increased PTIO. An additional batch of samplers with 30 % extra PTIO was deployed in the CATFAC in August 2024, and one with 100 % extra PTIO was deployed at the Marylebone site in February 2025.

3 Results

Results from the field and laboratory exposures are summarised in Table 1 and Table 2 respectively. Field exposures where the reference data did not meet the data capture requirements outlined in Section 2.2 (data capture > 85 %) are not included in Table 1 and were not used in any of the data analysis presented in this work. The field exposures that did not meet the data capture criterion were those for March 2023 (data capture = 68.6 %) and June 2024 (data capture = 52.9 %). All the laboratory exposures had data capture > 95 %. All travel blank samplers returned nitrite masses < 0.05 µg. The following sections illustrate the procedures followed to determine the sampling rate of the samplers under test, as well as the results of the storage and oxidant tests.

3.1 Data analysis procedure

The passive sampling mechanism for diffusion tubes is described by Fick's first law of diffusion. Accordingly, the NO_2 diffusive sampling rate, U_{NO_2}, in units of $m^3\ h^{-1}$, can be determined from Equation 1:

$$U_{NO_2} = \frac{m_{NO_2}}{[NO_2] \times t} \quad (1)$$

where m_{NO_2} is the mean mass of nitrite from NO_2 in µg, $[NO_2]$ is the mean NO_2 concentration over the exposure period measured by the reference instrument (either in the field or in the CATFAC) and reported in µg m^{-3} at standard temperature and pressure (293 K and 101.3 kPa), and t is the duration of the exposure in h.

Similarly, the NO diffusive sampling rate, U_{NO}, in units of $m^3\ h^{-1}$, can be determined from Equation 2:

$$U_{NO} = \frac{m_{NO_x} - m_{NO_2}}{[NO] \times t} \quad (2)$$

where m_{NO_x} is the mean mass of NO_x in µg reported as nitrite, m_{NO_2} is the mean mass of NO_2 in µg reported as nitrite, [NO] is the mean NO concentration over the exposure period measured by the reference instrument (either in the field or in the CATFAC), and reported in µg m^{-3} at standard temperature and pressure (293 K and 101.3 kPa), and t is the duration of the exposure period in h.

https://doi.org/10.5194/egusphere-2026-5280
Preprint. Discussion started: 16 November 2026
© Author(s) 2026. CC BY 4.0 License.

If exposures are carried out at standard temperature (*e.g.*, in the case of controlled laboratory exposures), the gradient of plots of mass of nitrite against the product of NO_2 or NO concentrations and the exposure time (often referred to as the dosage) corresponds to the diffusive sampling rate at standard temperature, $U(293\ \mathrm{K})$. When exposures are not performed at standard temperature (*e.g.*, in the case of field exposures), the same approach returns the diffusive sampling rate at the average temperature T across all exposures, $U(T)$. Previous studies (Butterfield et al., 2021; Martin et al., 2014) converted $U(T)$ to $U(293\ \mathrm{K})$ using the dependence of diffusive sampling rates on temperature (BS EN 16339:2025, 2025), described by the Equation (3):

$$U(T) = U(293\ \mathrm{K})\left(\frac{T}{293\ \mathrm{K}}\right)^{1.81} \qquad (3)$$

where T is the mean absolute temperature across all exposures. In this study, a different approach was taken. Instead of correcting the diffusive sampling rate to standard temperature, the masses of nitrite collected in each exposure, $m(T)$, were individually corrected to standard temperature, $m(293\ \mathrm{K})$, using Equation 4:

$$m(293\ \mathrm{K}) = m(T)/\left(\frac{T}{293\ \mathrm{K}}\right)^{1.81} \qquad (4)$$

This approach has the advantage of removing the effect of temperature variations on the data, thus allowing the investigation of the effect of environmental variables (other than ambient temperature) on the observed sampling rate. This is extensively discussed in Section 4.2.

To validate this approach, the sampling rates obtained from the nitrite masses normalised using Equation 4 were compared to those obtained from the raw nitrite masses (*i.e.*, not normalised to 20 °C) and then converted to standard conditions using Equation 3. The differences between the two sets were < 0.5 %, indicating the two approaches to the determination of the sampling rate are consistent with one another. Given the advantages of using the normalised nitrite masses (see above and Section 4.2), all the results described henceforth incorporate this correction.

Equations 1 and 2 were used to determine the experimental NO and NO_2 diffusive sampling rates for both Gradko and Passam NO_x samplers, using nitrite masses corrected to standard temperature. Lack-of-fit (linearity) plots for both types of diffusive samplers were produced using XLGENLINEv2, a generalised least-squares (GLS) routine employing a Microsoft Excel-based software package for low degree polynomial fitting developed at NPL (Smith, 2010). XLGENLINEv2 employed a user defined input file containing values of x and $u(x)$ (respectively the known NO_2 or NO concentrations multiplied by the exposure time and the combined standard uncertainty) together with y and $u(y)$ (respectively the reported mean mass of nitrite from NO_2 or NO, and its standard uncertainty, both normalised to 20 °C using Equation 4). The software package was used to perform a

https://doi.org/10.5194/egusphere-2026-5280
Preprint. Discussion started: 16 November 2026
© Author(s) 2026. CC BY 4.0 License.

first-order polynomial GLS fit, in this case forced through the origin. This was supported by the negligible masses collected by the travel blanks (< 0.05 µg), indicating no contamination had occurred during the measurement process. The fitted function automatically calculated analytical results with defined uncertainties for the data.

https://doi.org/10.5194/egusphere-2026-5280
Preprint. Discussion started: 16 November 2026
© Author(s) 2026. CC BY 4.0 License.

Table 1 Results from field exposures. Each mass of nitrite represents the average of five replicates and is accompanied by the value of one standard deviation within each set of replicates. Note that raw masses of nitrite are reported, *i.e.* not normalised to 20 °C.

Exposure period	Reference NO_2 / μg m^{-3}	Reference NO / μg m^{-3}	Data capture / %	Mass of nitrite / μg				Reference O_3 / μg m^{-3}	Ambient temperature / °C	Wind speed / m s^{-1}
				Gradko NO_2	Gradko NO_x	Passam NO_2	Passam NO_x			
02/11/2022-30/11/2022	46.99	41.13	99.9	2.03 ± 0.17	2.54 ± 0.08	-	-	16.20	11.9	0.34
30/11/2022-04/01/2023	42.10	32.28	99.6	2.25 ± 0.07	2.74 ± 0.10	-	-	20.17	6.9	0.44
04/01/2023-01/02/2023	46.99	41.38	99.1	1.99 ± 0.12	2.51 ± 0.16	1.33 ± 0.04	2.77 ± 0.12	22.74	7.2	0.39
01/02/2023-01/03/2023	44.57	42.51	99.6	1.99 ± 0.08	2.59 ± 0.17	1.37 ± 0.04	2.84 ± 0.08	23.00	8.6	0.46
05/04/2023-03/05/2023	39.31	16.51	92.7	1.74 ± 0.04	1.85 ± 0.10	1.21 ± 0.05	1.98 ± 0.12	43.50	11.5	0.51
03/05/2023-31/05/2023	31.96	13.15	99.4	1.32 ± 0.02	1.53 ± 0.02	0.88 ± 0.05	1.35 ± 0.06	43.76	14.7	0.51
31/05/2023-05/07/2023	39.12	18.48	99.5	2.13 ± 0.04	2.22 ± 0.07	1.45 ± 0.03	1.92 ± 0.09	42.78	20.0	0.49
05/07/2023-02/08/2023	37.45	30.41	96.6	1.72 ± 0.03	2.05 ± 0.06	1.21 ± 0.04	2.03 ± 0.14	21.17	19.7	0.34
03/08/2023-07/09/2023	38.18	25.25	99.4	1.95 ± 0.05	2.30 ± 0.03	1.43 ± 0.05	2.46 ± 0.15	26.57	19.5	0.29
06/09/2023-04/10/2023	51.57	33.31	99.0	2.24 ± 0.10	2.40 ± 0.12	1.52 ± 0.07	2.51 ± 0.06	27.82	19.7	0.26
04/10/2023-01/11/2023	51.24	35.78	99.4	2.01 ± 0.10	2.25 ± 0.16	1.43 ± 0.04	2.36 ± 0.15	17.01	17.3	0.28

01/11/2023-06/12/2023	41.96	33.92	95.5	2.16 ± 0.04	2.68 ± 0.15	1.54 ± 0.07	3.22 ± 0.49	17.64	8.9	0.35
05/12/2023-02/01/2024	42.22	31.19	98.8	1.69 ± 0.03	2.15 ± 0.14	1.24 ± 0.05	2.16 ± 0.08	29.51	10.6	0.47
03/01/2024-31/01/2024	42.51	27.14	99.0	1.61 ± 0.06	1.98 ± 0.09	-	-	29.55	6.7	0.20
31/01/2024-06/03/2024	48.81	31.76	99.6	2.23 ± 0.06	2.62 ± 0.13	1.73 ± 0.09	2.77 ± 0.14	30.35	9.9	0.44
06/03/2024-03/04/2024	42.14	23.80	99.4	1.64 ± 0.01	1.98 ± 0.10	1.24 ± 0.01	2.02 ± 0.05	35.03	11.1	0.43
03/04/2024-01/05/2024	31.08	17.24	99.0	1.33 ± 0.05	1.50 ± 0.02	1.04 ± 0.03	1.62 ± 0.08	48.54	11.9	0.50
01/05/2024-05/06/2024	32.97	20.29	96.6	1.94 ± 0.03	2.24 ± 0.19	1.49 ± 0.05	2.20 ± 0.15	41.99	16.2	0.37
03/07/2024-31/07/2024	33.88	23.02	99.4	1.67 ± 0.04	1.72 ± 0.06	1.10 ± 0.03	1.82 ± 0.09	30.88	19.7	0.23
31/07/2024-04/09/2024	29.50	19.40	98.7	2.14 ± 0.05	2.43 ± 0.14	1.41 ± 0.06	2.10 ± 0.15	33.19	20.6	0.17
04/09/2024-02/10/2024	30.76	19.81	94.5	1.50 ± 0.03	1.73 ± 0.06	0.97 ± 0.03	1.61 ± 0.05	31.73	15.9	0.37
02/10/2024-06/11/2024	37.55	30.59	99.6	2.13 ± 0.08	2.39 ± 0.12	1.51 ± 0.06	3.02 ± 0.06	18.83	14.0	0.27
06/11/2024-04/12/2024	37.29	32.87	99.1	1.60 ± 0.04	2.10 ± 0.19	1.22 ± 0.01	2.48 ± 0.06	19.77	9.4	0.37
04/12/2024-08/01/2025	32.55	23.59	99.4	1.91 ± 0.10	2.32 ± 0.18	1.32 ± 0.02	2.40 ± 0.11	28.99	8.2	0.61

https://doi.org/10.5194/egusphere-2026-5280
Preprint. Discussion started: 16 November 2026
© Author(s) 2026. CC BY 4.0 License.

08/01/2025-05/02/2025	43.33	39.22	97.3	1.90 ± 0.04	2.68 ± 0.23	1.38 ± 0.04	2.71 ± 0.09	19.56	7.6	0.35
05/02/2025-05/03/2025	34.50	21.95	95.7	1.71 ± 0.04	2.01 ± 0.22	-	2.03 ± 0.05	28.20	7.2	0.90
05/03/2025-02/04/2025	35.09	17.27	99.7	1.48 ± 0.06	1.97 ± 0.07	1.12 ± 0.02	1.84 ± 0.07	39.48	10.6	NA

285 **Table 2 Results from laboratory exposures. Each mass of nitrite represents the average of five replicates and is accompanied by the value of one standard deviation within each set of replicates.**

Exposure period	Reference NO_2 / µg m^{-3}	Reference NO / µg m^{-3}	Data capture / %	Mass of nitrite / µg			
				Gradko NO_2	Gradko NO_x	Passam NO_2	Passam NO_x
06/03/2023-31/03/2023	46.61	27.93	99.9	1.98 ± 0.05	2.39 ± 0.08	1.20 ± 0.06	2.22 ± 0.05
05/05/2023-02/06/2023	39.47	41.75	99.9	1.80 ± 0.06	2.77 ± 0.18	1.13 ± 0.03	2.86 ± 0.03
26/10/2023-21/11/2023	45.73	25.66	99.9	1.80 ± 0.15	2.49 ± 0.20	1.30 ± 0.07	2.44 ± 0.15
01/12/2023-29/12/2023	33.54	13.43	99.9	1.73 ± 0.19	2.30 ± 0.22	1.28 ± 0.09	1.93 ± 0.08
08/03/2024-05/04/2024	6.04	49.08	99.9	0.31 ± 0.06	1.35 ± 0.15	0.17 ± 0.01	2.61 ± 0.04
26/07/2024-23/08/2024	30.24	33.60	99.9	1.30 ± 0.01	1.79 ± 0.07	0.82 ± 0.02	2.05 ± 0.04

https://doi.org/10.5194/egusphere-2026-5280
Preprint. Discussion started: 16 November 2026
© Author(s) 2026. CC BY 4.0 License.

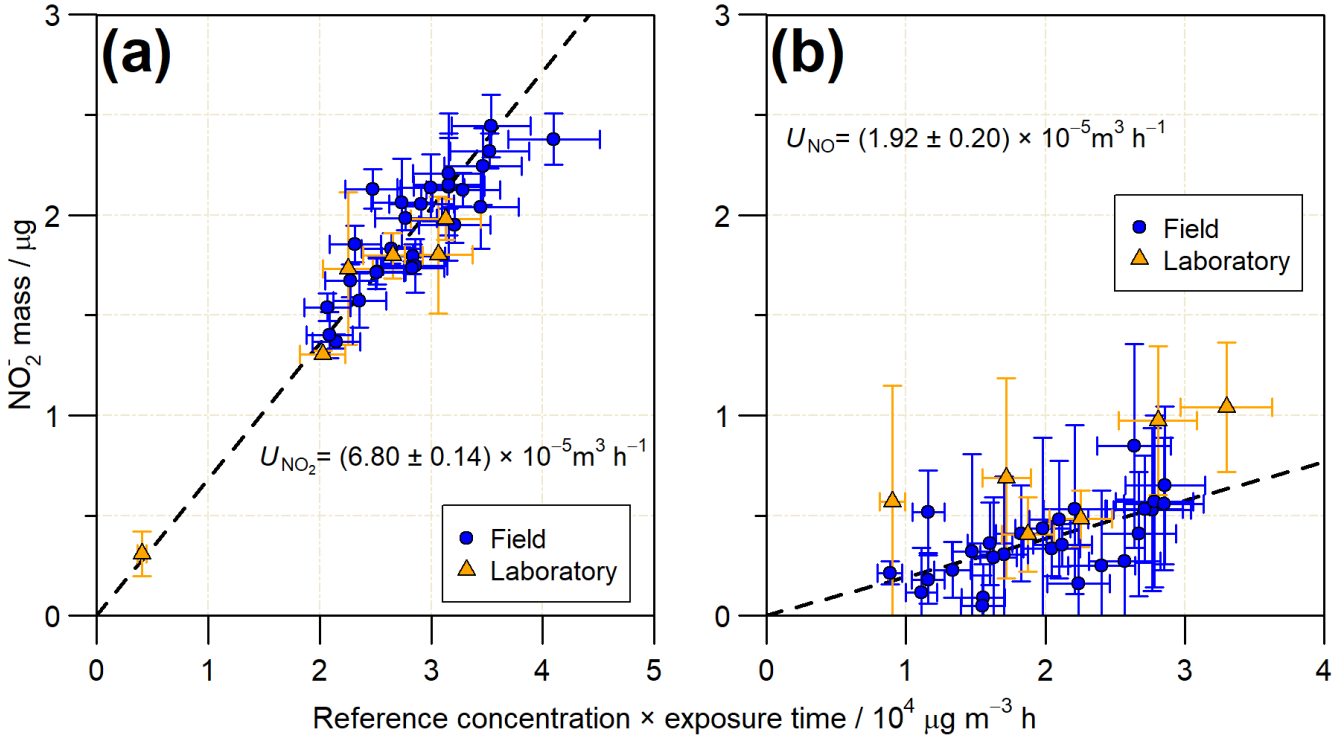
https://doi.org/10.5194/egusphere-2026-5280
Preprint. Discussion started: 16 November 2026
© Author(s) 2026. CC BY 4.0 License.

3.2 Diffusive sampling rate results

Figure 4 and Figure 5 show the lack-of-fit plots for Gradko's and Passam's diffusive samplers, respectively. In Figure 4a and Figure 5a, the average mass of nitrite from the analysis of exposed NO_2 samplers (normalised for temperature) is plotted on the *y*-axis, and the product of the NO_2 reference concentration and exposure time is plotted on the *x*-axis. In Figure 4b and Figure 5b, the average mass of nitrite (in this case the difference in mass between the NO_x and NO_2 samplers, also normalised for temperature) is plotted on the *y*-axis, and the product of the NO reference concentration and exposure time is plotted on the *x*-axis.

The error bars shown in the graphs represent the estimated uncertainties. The uncertainty in the mass of nitrite was calculated as the standard deviation of each set of five samplers (as shown in Table 1 and Table 2). Just as the mass of nitrite, the uncertainty was also normalised for the effect of temperature. The uncertainty in the *x*-axis is dominated by the uncertainty in the NO or NO_2 reference concentrations. Typically, these carry a maximum of 15 % expanded uncertainty (Department for Environment, Food & Rural Affairs, 2023). This is the criterion required to meet the data quality objectives of the European Union and UK legislation (EU Directive 2008/50/EC, 2008; EU Directive 2024/2881, 2024). In this work, we estimated that the random component of the uncertainty in the reference method becomes vanishingly small when the hourly measurements are averaged to produce four- or five-week means (corresponding to the exposure period), resulting in an expanded uncertainty of 10 % in the reported reference NO and NO_2 concentrations (Butterfield et al., 2021).

https://doi.org/10.5194/egusphere-2026-5280
Preprint. Discussion started: 16 November 2026
© Author(s) 2026. CC BY 4.0 License.



305

Figure 4: Plots of mass of nitrite collected from Gradko diffusive samplers (normalised to 20 °C) against the product of reference concentration and exposure time for a) NO_2 and b) NO. The gradient of the line of best fit (dashed back line) through both field and laboratory data is the diffusive sampling rate, *U*. Vertical error bars represent two standard deviations within each exposure of five replicate samplers, whilst horizontal error bars reflect the estimated expanded uncertainty (10 %) in the reference concentrations.

https://doi.org/10.5194/egusphere-2026-5280
Preprint. Discussion started: 16 November 2026
© Author(s) 2026. CC BY 4.0 License.

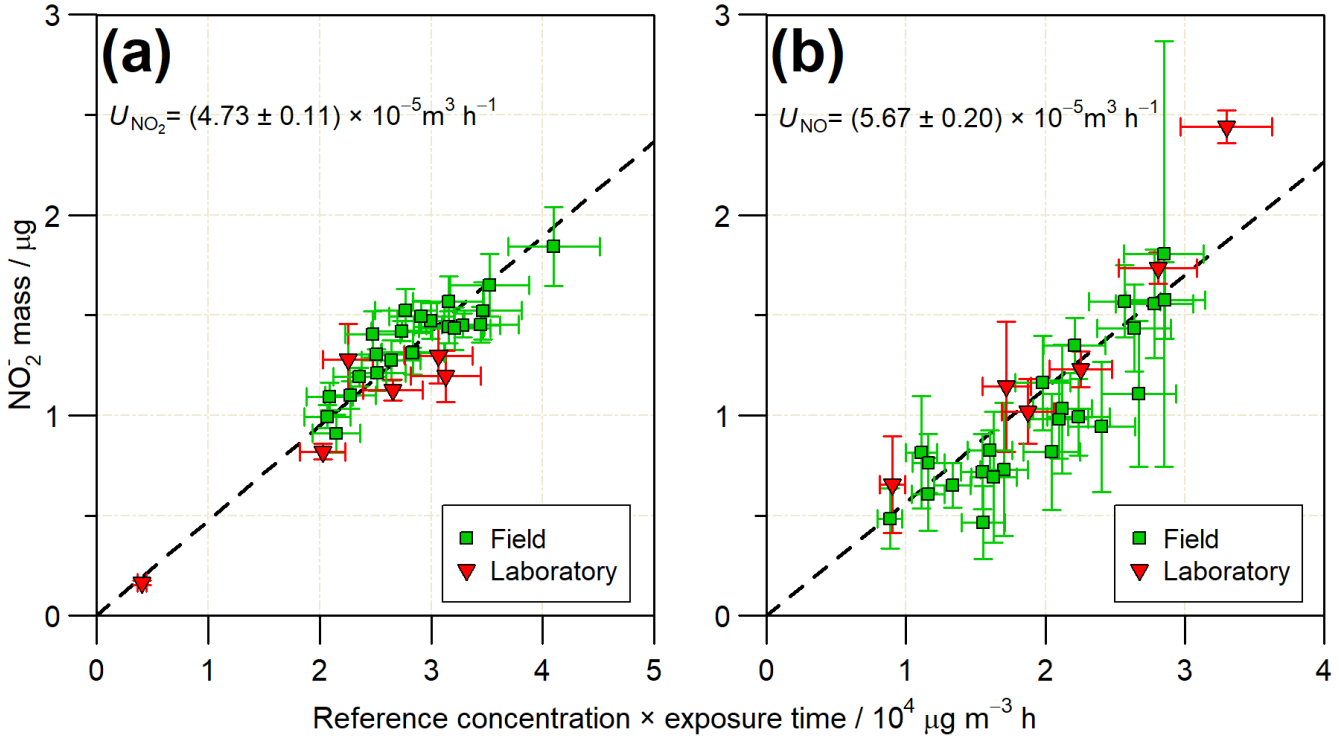


Figure 5: Plots of mass of nitrite collected from Passam diffusive samplers (normalised to 20 °C) against the product of reference concentration and exposure time for a) NO_2 and b) NO. The gradient of the line of best fit (dashed back line) through both field and laboratory data is the diffusive sampling rate, *U*. Vertical error bars represent two standard deviations within each exposure of five replicate samplers, whilst horizontal error bars reflect the estimated expanded uncertainty (10 %) in the reference concentrations.

The NO_2 and NO diffusive sampling rates for both types of samplers were determined from the gradients of the straight-line fits to the plots incorporating both field and laboratory data. As the reference concentrations are reported at standard temperature and pressure (T = 20 °C and p = 101.3 kPa) and the nitrite masses were normalised to 20 °C, all reported diffusive sampling rates are also reported at those standard conditions.

U_{NO_2} for Gradko samplers prepared with 50 % TEA/acetone is (6.80 ± 0.14) × 10^{-5} m^3 h^{-1}, within the measurement uncertainty of U_{NO_2} for samplers prepared with 20 % TEA/H_2O in previous studies, *e.g.*, (6.64 ± 0.66) × 10^{-5} m^3 h^{-1} (Martin et al., 2014) and (6.68 ± 0.46) × 10^{-5} m^3 h^{-1} (Butterfield et al., 2021), as reported in Table 3. U_{NO} was determined as (1.92 ± 0.20) × 10^{-5} m^3 h^{-1}.

https://doi.org/10.5194/egusphere-2026-5280
Preprint. Discussion started: 16 November 2026
© Author(s) 2026. CC BY 4.0 License.

In the case of Passam, the new traceable determinations of U_{NO} and U_{NO_2} presented here are (5.67 ± 0.20) × 10^{-5} and (4.73 ± 0.11) × 10^{-5} m^3 h^{-1} respectively. These are in good agreement with previous in-house measurements by Passam (Passam AG, 2020), U_{NO} = (5.74 ± 1.72) × 10^{-5} m^3 h^{-1} and U_{NO_2} = (4.46 ± 1.32) × 10^{-5} m^3 h^{-1}, with lower uncertainties in the current study.

Sampling rates from previous studies and this work are summarised in Table 3. For NO_x and NO_2 diffusive samplers of identical dimensions, assuming the conversion efficiency of NO to NO_2 is 100 %, the ratio of U_{NO} and U_{NO_2} should be commensurate to the ratio of the diffusivities of NO and NO_2 in air, 0.1802 and 0.1361 cm s^{-1} respectively (Massman, 1998). This theoretical ratio is 1.32 ± 0.47. While the reference values for the diffusivities are reported at standard conditions (T = 0 °C and p = 101.3 kPa), correcting them for T = 20 °C would not alter the value of their ratio. The ratio of sampling rates for the Passam tubes from this work is 1.21 ± 0.05, in good agreement (within the stated uncertainties) with both the theoretical ratio of diffusivities and a previous in-house determination by the manufacturer (1.29 ± 0.55). However, the ratio of sampling rates for the Gradko tubes is significantly different (0.29 ± 0.03) from the theoretical ratio. This led to further work investigating the oxidation efficiency of the Gradko samplers (see Section 3.4).

Table 3 Summary of sampling rates results at standard condition (T = 20 °C and p = 101.3 kPa).

Sampler type	U_{NO_2} / 10^{-5} m^3 h^{-1}	U_{NO} / 10^{-5} m^3 h^{-1}	U_{NO}/U_{NO_2}
Gradko 50 % TEA/acetone (this work)	6.80 ± 0.14	1.92 ± 0.20	0.28 ± 0.03
Gradko 20 % TEA/H_2O (Martin et al., 2014)	6.64 ± 0.66		
Gradko 20 % TEA/H_2O (Butterfield et al., 2021)	6.68 ± 0.46		
Passam (this work)	4.73 ± 0.11	5.67 ± 0.20	1.20 ± 0.05
Passam (in-house) (Passam AG, 2020)	4.46 ± 1.32	5.74 ± 1.72	1.29 ± 0.55
Theoretical from NO and NO_2 diffusivities (Massman, 1998)			1.32 ± 0.47

https://doi.org/10.5194/egusphere-2026-5280
Preprint. Discussion started: 16 November 2026
© Author(s) 2026. CC BY 4.0 License.

3.3 Storage tests

Results from the storage tests are illustrated in Figure 6 and Figure 7 for Gradko and Passam samplers, respectively. A significance analysis (Ferracci et al., 2015; Martin et al., 2019) was performed on the temporal trends shown in Figure 6a and Figure 7a to establish if any change in collected nitrite with storage time was statistically significant in the light of the uncertainties associated with the data points. Weighted least squares fits to the plots of mass of nitrite against storage time were performed using XLGENLINEv2. In all cases, with the exception of NO_x Passam samplers stored over two months, the values of the gradients obtained overlap with zero within their expanded uncertainties (k = 2), indicating no statistically significant loss of nitrite across the duration of the tests (Figure 6b and Figure 7b). Similarly, all storage tests (with the exception of NO_x Passam samplers stored over two months) showed losses in mass of nitrite (if any) smaller than the 10 % tolerance typically applied to diffusive samplers (BS EN 13528-2:2002, 2002).

As for the NO_x Passam samplers stored over two months, the uncertainty interval in the corresponding gradient only narrowly misses its overlap with zero. However, the repeat of the same test a few months later with a longer storage time (three months) showed no statistically significant decrease in nitrite after storage. Other factors, such as an underestimate of the uncertainties in the retrieved mass of nitrite, may have affected these results. Users are however encouraged to limit storage times and return exposed samples for analysis at their earliest convenience.

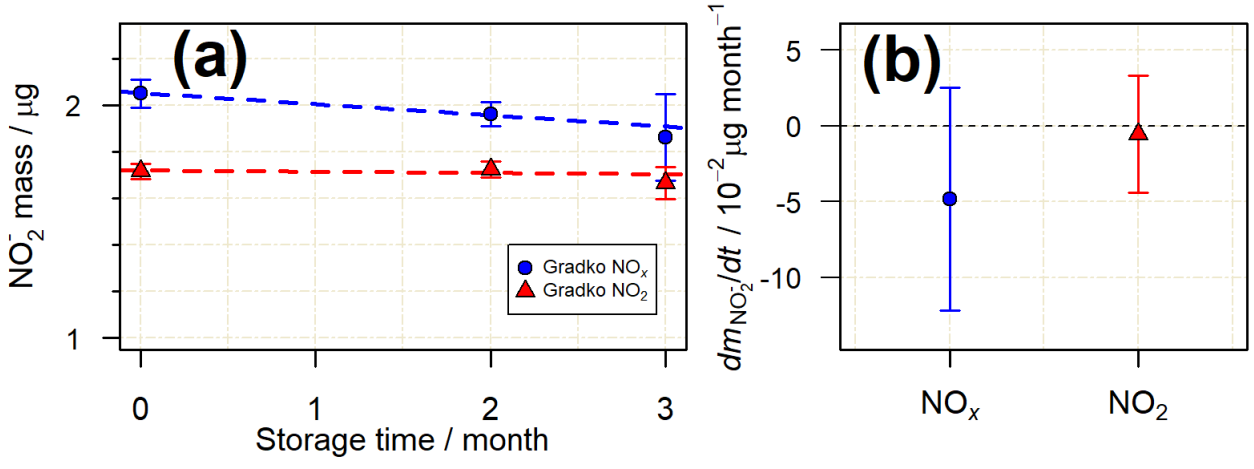


Figure 6: Storage test results for Gradko NO_x and NO_2 samplers. a) mean mass of collected nitrite from both types of samplers during the storage tests as a function of storage time. Error bars indicate one standard deviation within each set of five replicates. Lines of best fit (dashed coloured lines) are weighted for the uncertainty in the mass of nitrite. b) Significance analysis on the gradients of the lines of best fit from panel a). Error bars represent the expanded uncertainty (k = 2) in the gradients. Overlap of the error bars with zero (dashed black line) indicates no statistically significant loss of nitrite across the 3 months.

https://doi.org/10.5194/egusphere-2026-5280
Preprint. Discussion started: 16 November 2026
© Author(s) 2026. CC BY 4.0 License.

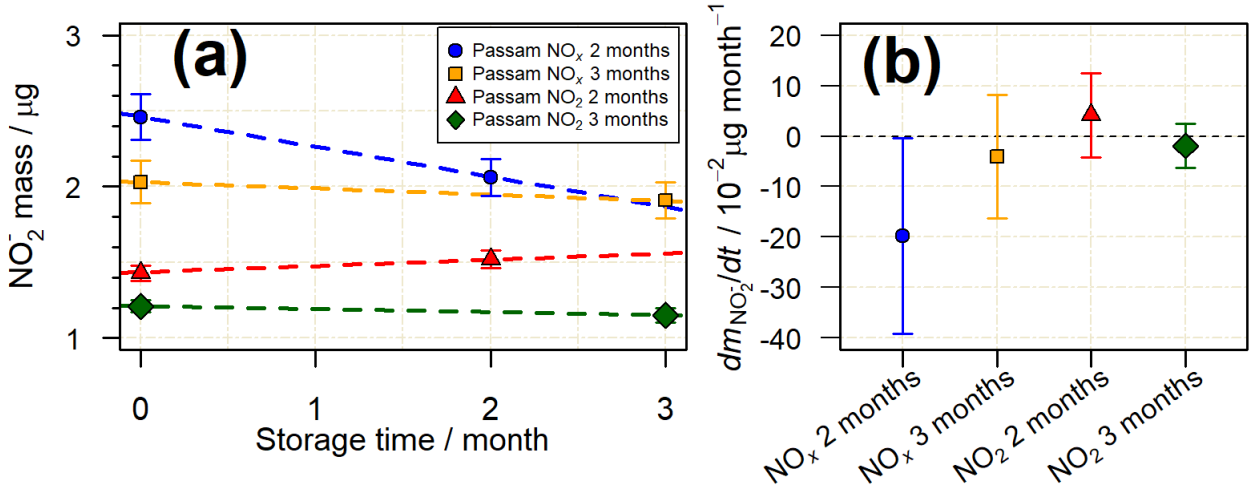


Figure 7: Storage test results for Passam NO_x and NO_2 samplers. a) mean mass of collected nitrite from both types of samplers during the storage tests as a function of storage time. Error bars indicate one standard deviation within each set of five replicates. Lines of best fit (dashed coloured lines) are weighted for the uncertainty in the mass of nitrite. b) Significance analysis on the gradients of the lines of best fit from panel a). Error bars represent the expanded uncertainty ($k = 2$) in the gradients. Overlap of the error bars with zero (dashed black line) indicates no statistically significant loss of nitrite across the duration of the tests.

3.4 Oxidant test results

As described in Section 3.2, the NO diffusive sampling rate for the Gradko samplers is a factor of 4-5 lower than the ratio of NO/NO_2 diffusivities would lead to expect. This could be due to incomplete conversion of NO into NO_2. To investigate this hypothesis, Gradko provided additional batches of NO_x samplers in which larger amounts of PTIO oxidant had been added relative to the standard sampler. An additional batch with ~30 % more oxidant was deployed in a laboratory exposure, along with a standard set of samplers, in August 2024 and collected 32 % more nitrite from NO (0.64 ± 0.15 µg) than the batch with the standard amount of oxidant (0.48 ± 0.07 µg). A further additional batch with ~100 % additional oxidant was deployed at the Marylebone site in February 2025 and collected 87 % more nitrite from NO (0.55 ± 0.29 µg) than the batch with the standard amount of oxidant (0.29 ± 0.22 µg).

These results indicate that amount of nitrite collected from NO varies more or less linearly with the amount of oxidant, and that the amount of oxidant present in the standard version of the samplers may not be sufficient to ensure 100 % conversion of NO into NO_2 throughout the exposure period. The potential implications of this are discussed in the following section.

https://doi.org/10.5194/egusphere-2026-5280
Preprint. Discussion started: 16 November 2026
© Author(s) 2026. CC BY 4.0 License.

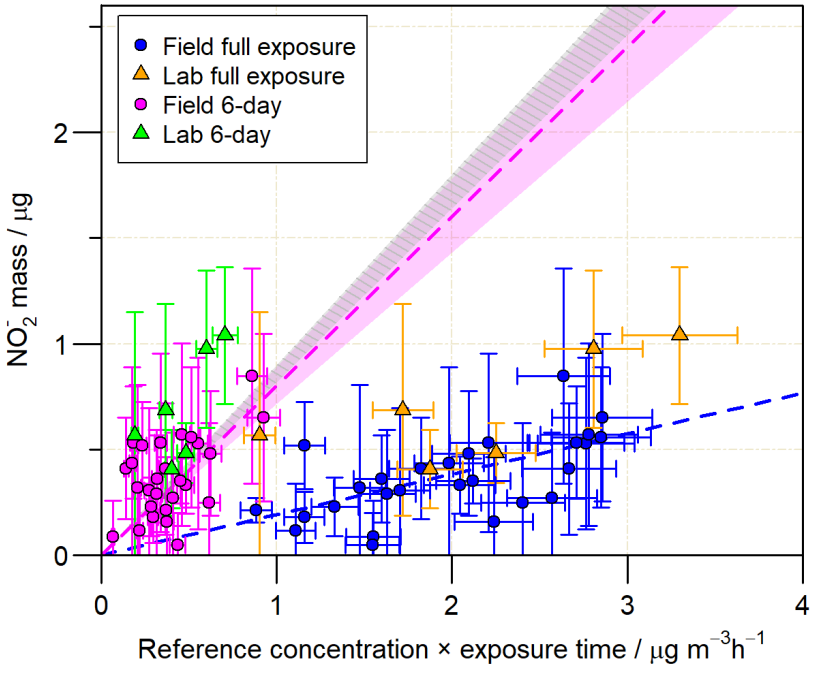


Figure 8: Analysis of collected nitrite mass (from NO) for Gradko NO_x samplers using different lengths of exposure time: the full duration (four or five weeks, blue circles and orange triangles) and six days (pink circles and green triangles). The dashed blue line represents the line of best fit through the full exposure period data (same as in Figure 4). The grey hatched area represents gradients (*i.e.*, NO sampling rates) over the expected range (7.9-8.6) × 10^{-5} m^3 h^{-1}. The dashed pink line represents the line of best fit through the simulated 6-day exposure data, and the pink shaded area its expanded uncertainty range (k = 2).

4 Discussion

4.1 Simulating oxidant depletion

Based on the value of U_{NO_2} for the Gradko samplers of (6.80 ± 0.14) × 10^{-5} m^3 h^{-1}, and on values of the ratio between U_{NO} and U_{NO_2} in the range 1.20 to 1.32 (Table 3), the expected value of U_{NO} for the Gradko samplers should be in the range of (8.2-9.0) × 10^{-5} m^3 h^{-1}, provided conversion of NO to NO_2 was 100 % efficient. Instead, the observed U_{NO} for Gradko samplers was (1.92 ± 0.20) × 10^{-5} m^3 h^{-1}. Further tests highlighted that the mass of collected nitrite originating from NO varied linearly with the amount of oxidant, indicating the PTIO was not present in sufficient amounts to guarantee oxidation to NO_2 throughout the exposure period for both lab and field tests (Section 3.4). Nitrite masses collected from Gradko NO_x samplers were reanalysed by simulating the oxidant becoming depleted well before the end of the exposure period. The oxidant was estimated to become depleted after ~six days, *i.e.* ~22 % of a typical 28-day exposure period, based on the observed sampling rate being approximately 22 % of the expected value. Mean reference NO concentrations were recalculated across the first six days of each exposure, and this resulted in a new plot of the average mass of nitrite from NO samplers against the product of the six-day mean reference NO concentration and exposure time. This is shown in Figure 8 along with the previous analysis of the

https://doi.org/10.5194/egusphere-2026-5280
Preprint. Discussion started: 16 November 2026
© Author(s) 2026. CC BY 4.0 License.

NO nitrite data across the full exposure periods. The reanalysed data, effectively simulating a six-day exposure, return a gradient of (8.02 ± 0.87) × 10^{-5} m^3 h^{-1} (pink dashed line and shaded area in Figure 8). This value is consistent (within its uncertainty) with U_{NO} in the expected range of (8.2-9.0) × 10^{-5} m^3 h^{-1} (indicated by the grey hatched area in Figure 8). This analysis makes a crucial assumption on the timescale of oxidant depletion, which may deviate from the assumed value of six days (*e.g.*, depletion may occur sooner during exposure periods of high NO, and *vice versa*). This would directly affect the gradient of the simulated shorter exposure periods. This analysis is however consistent with oxidant depletion as the cause of the low values of U_{NO} for the Gradko samplers.

4.2 Effect of environmental and chemical variables on the diffusive sampling rates

Results were also analysed to assess the effects of environmental variables (*e.g.*, temperature, wind speed) and chemical processes (*e.g.*, reaction of NO with O_3 along the diffusion pathlength, and sorbent saturation in the presence of high concentrations of the analytes) on the diffusive sampling rates. To achieve this, individual sampling rates were calculated from each exposure, be it in the field or in the laboratory, dividing the collected mass of nitrite by the product of the reference concentration and the exposure time. This is equivalent to evaluating the gradient of lines between the origin and each individual data point in Figure 4 and Figure 5. These values of the sampling rate were then plotted against analyte concentration, temperature, wind speed and ozone concentrations, as shown in Figure 9 and Figure 10. A GLS linear fit was determined for each plot, along with its 95 % confidence interval.

Focusing on the variation of sampling rate with analyte concentration in panels (a) and (e) of Figure 9 and Figure 10, there appear to be signs of sorbent saturation for the NO_2 samplers from both suppliers, with lower sampling rates observed at high [NO_2]. However, this trend is only statistically significant for the NO_2 Gradko samplers (Figure 9a). No statistically significant effect of [NO] on sampling rate was observed for NO_x samplers from either supplier. In the case of the Gradko NO_x samplers, this behaviour is still consistent with the depletion of the oxidant, as the mass of nitrite collected from NO in the sample is limited by the availability of the oxidant.

As discussed in Section 3.1, the dependence of diffusive sampling rates on temperature is well documented in the literature (BS EN 16339:2025, 2025). With this in mind, the procedure adopted to normalise the collected nitrite masses to standard temperature (20 °C) has successfully removed any effect of temperature on the observed sampling rates, as none of the trends in panels (b) and (f) in Figure 9 and Figure 10 is statistically significant.

All the samplers tested are equipped with wind caps, which have been demonstrated to reduce the positive bias introduced by turbulence at the inlet at high wind speeds (resulting in a shortening of the diffusive pathlength and therefore higher observed sampling rates). The Passam samplers were also housed in a protective shelter during the exposures in the field, which further limited the effect of wind (Medland et al., 2025). The variation of sampling rate with wind speed is shown in panels (c) and

https://doi.org/10.5194/egusphere-2026-5280
Preprint. Discussion started: 16 November 2026
© Author(s) 2026. CC BY 4.0 License.

(g) of Figure 9 and Figure 10. No statistically significant trend can be identified for the NO_2 samplers in panel (c), whereas a statistically significant positive gradient is observed for NO from both suppliers. It must be noted that the data points from laboratory exposures significantly bias the linear fit performed with the full dataset (black line and grey shaded area). As discussed below, the laboratory exposures were performed in the complete absence of ozone, which would otherwise remove NO from the sampled air over the diffusion timescales between the sampler inlet and the sorbent. The higher sampling rates observed for laboratory exposures relative to the field exposures are therefore potentially affected by the lack of ozone. When only the field data are used (blue line and shaded area in Figure 9, green line and shaded area in Figure 10), the observed trends become statistically insignificant.

The residence time within the samplers is ~9 min for NO_2 and ~7 min for NO. This is sufficient time to allow for some of the NO and O_3 in ambient air to react along the diffusive pathway to generate NO_2. Previous work on non-wind-capped samplers has shown this could contribute to an overestimation of NO_2 > 20 % (Heal et al., 1999; Heal and Cape, 1997). If this was the case in the present study, then NO sampling rates derived from exposures at high O_3 levels would be lower than those at low O_3 levels. By contrast, the opposite would occur for NO_2, with sampling rates higher for high O_3 exposures as some of the NO in the air is converted to NO_2 by in-tube chemistry, and lower for those at low O_3 concentrations. Our dataset has the unique advantage of not only having field exposures across a wide range of ozone concentrations (15 – 50 µg m^{-3}), but all laboratory exposures were carried out in the complete absence of O_3.

Of the relationships between sampling rate and [O_3] shown in panels d) and h) in Figure 9 and Figure 10, only the trend between the NO sampling rate and [O_3] for the Gradko samplers is statistically signifcant. However, we can still examine and compare the sampling rates under different ozone conditions: high ozone ([O_3] ≥ 30 µg m^{-3}), low ozone (0 < [O_3] < 30 µg m^{-3}), and no ozone (laboratory exposures). For Passam samplers, the average NO sampling rate was 5.00×10^{-5} m^3 h^{-1} at high ozone, 5.24×10^{-5} m^3 h^{-1} at low ozone, and 6.40×10^{-5} m^3 h^{-1} under no ozone conditions. By contrast, the average NO_2 sampling rate followed the opposite trend, with values of 4.88×10^{-5} m^3 h^{-1} at high [O_3], 4.77×10^{-5} m^3 h^{-1} at low [O_3] and 4.35×10^{-5} m^3 h^{-1} under no O_3. This behaviour is consistent with conversion of NO into NO_2 *via* reaction with O_3. A similar behaviour is observed for the Gradko samplers. The average Gradko NO sampling rate was 1.77×10^{-5} m^3 h^{-1} at high [O_3], 1.93×10^{-5} m^3 h^{-1} at low [O_3], and 3.54×10^{-5} m^3 h^{-1} under no O_3 conditions. On the other hand, the average NO_2 sampling rate was 6.88×10^{-5} m^3 h^{-1} at high [O_3], 6.77×10^{-5} m^3 h^{-1} at low [O_3] and 6.79×10^{-5} m^3 h^{-1} under no O_3.

https://doi.org/10.5194/egusphere-2026-5280
Preprint. Discussion started: 16 November 2026
© Author(s) 2026. CC BY 4.0 License.

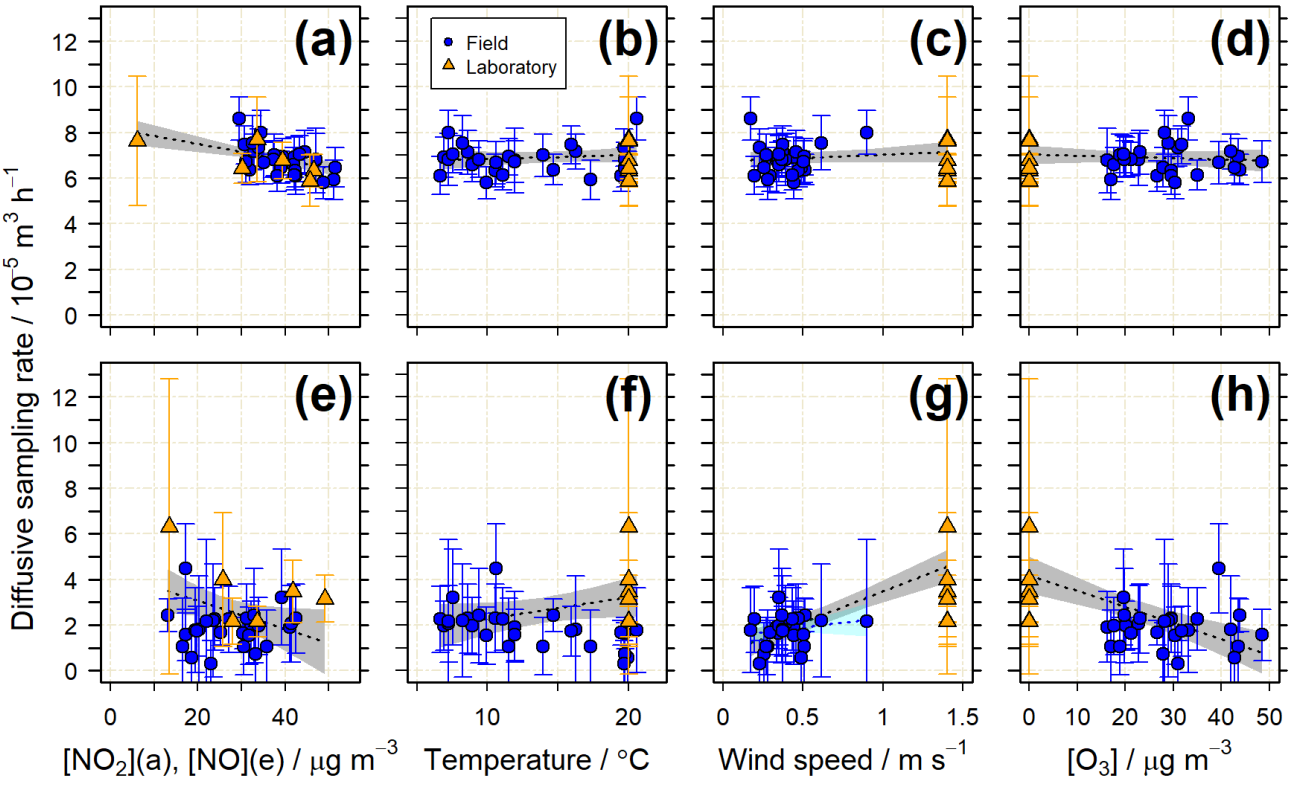


Figure 9: Analysis of diffusive sampling rates derived from individual exposures of Gradko samplers for NO_2 (top row, panels a, b, c, and d) and for NO (bottom row, panels e, f, g, and h). The diffusive sampling rates are plotted against target pollutant concentration (panel a for NO_2, panel e for NO), ambient temperature (panels b and f), wind speed (panels c and g) and ozone concentration (panels d and h). The black dashed lines represent the GLS linear fit to the data in each panel, with their 95 % confidence intervals (grey shaded areas). The blue dashed line in panel (g) represents the GLS fit to the field data only, with its 95 % confidence interval (blue shaded area).

https://doi.org/10.5194/egusphere-2026-5280
Preprint. Discussion started: 16 November 2026
© Author(s) 2026. CC BY 4.0 License.

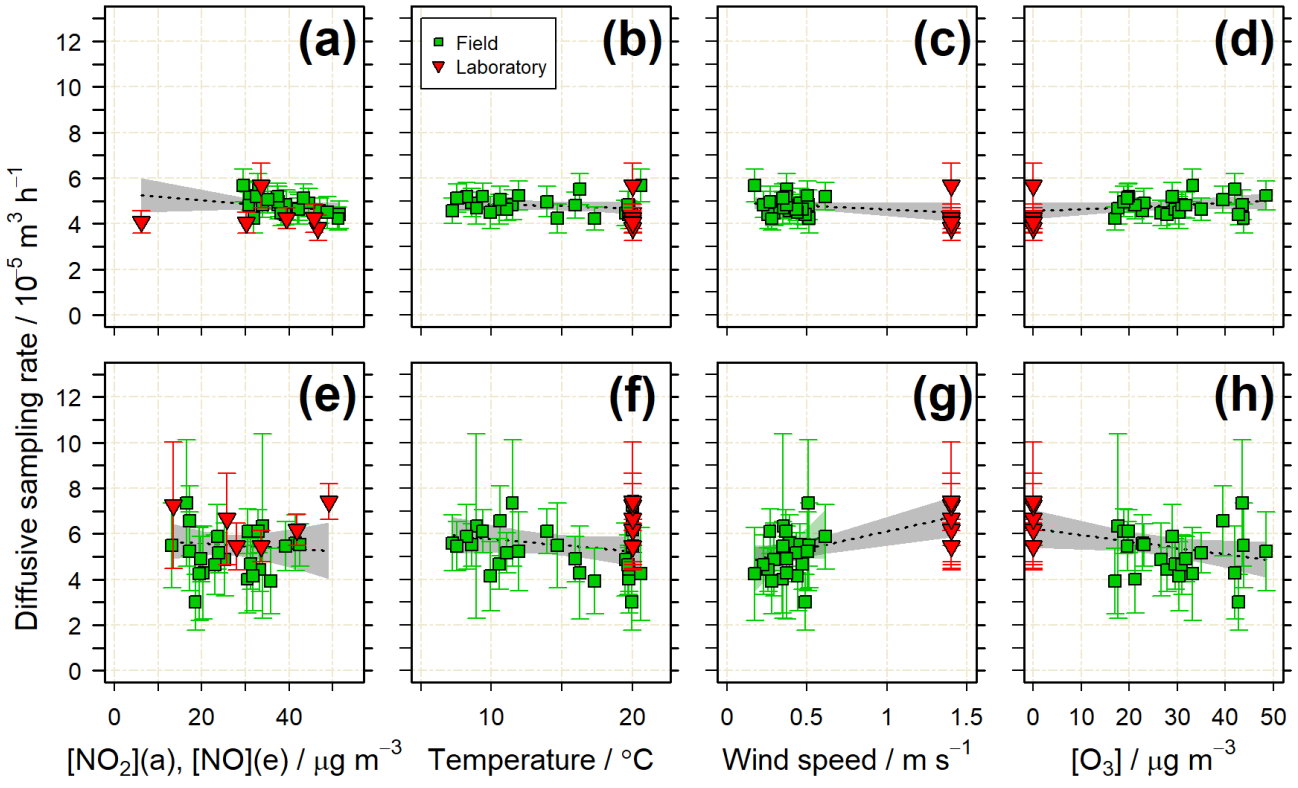


Figure 10: Analysis of diffusive sampling rates derived from individual exposures of Passam samplers for NO_2 (top row, panels a, b, c, and d) and for NO (bottom row, panels e, f, g, and h). The diffusive sampling rates are plotted against target pollutant concentration (panel a for NO_2, panel e for NO), ambient temperature (panels b and f), wind speed (panels c and g) and ozone concentration (panels d and h). The black dashed lines represent the GLS linear fit to the data in each panel, with their 95 % confidence intervals (grey shaded areas). The green dashed line in panel (g) represents the GLS fit to the field data only, with its 95 % confidence interval (green shaded area).

5 Summary and conclusions

This study presents a comprehensive validation of diffusive samplers for the simultaneous measurement of NO and NO_2. Through a combination of laboratory exposures in the Controlled Atmosphere Test Facility (CATFAC) and multi-year field deployments at the Marylebone Road air quality supersite, traceable diffusive sampling rates were determined for NO and NO_2 for samplers supplied by Gradko International and Passam AG.

The NO_2 sampling rate determined for the newly developed Gradko sampler prepared with a 50 % TEA/acetone coating was $U_{NO_2} = (6.80 \pm 0.14) \times 10^{-5}$ m^3 h^{-1}, in agreement with values previously reported for earlier Gradko NO_2 diffusion tube designs with 20 % TEA/H_2O coating. This indicates that different sorbent recipe had no measurable effect on the NO_2 sampling rate. The corresponding NO sampling rate was determined as $U_{NO} = (1.92 \pm 0.20) \times 10^{-5}$ m^3 h^{-1}.

https://doi.org/10.5194/egusphere-2026-5280
Preprint. Discussion started: 16 November 2026
© Author(s) 2026. CC BY 4.0 License.

For the Passam samplers, sampling rates of U_{NO_2} = (4.73 ± 0.11) × 10^{-5} m^3 h^{-1} and U_{NO} = (5.67 ± 0.20) × 10^{-5} m^3 h^{-1} were obtained, consistent with previous measurements reported by the manufacturer and with theoretical expectations derived from molecular diffusivities.

Additional investigations demonstrated that adsorbed nitrite remains stable for at least two to three months when the exposed samplers are stored refrigerated prior to analysis. This provides confidence that routine transport and analytical delays are unlikely to introduce significant bias. Environmental analyses indicated that the adopted temperature normalisation successfully removed temperature-related effects on sampling rates. Wind effects were largely mitigated by the use of wind-protective caps and shelters, although evidence was found that ambient ozone may influence the apparent NO and NO_2 sampling rates through in-tube chemistry. These effects warrant further investigation, particularly for applications in environments with elevated ozone concentrations.

The NO sampling rate observed for the Gradko samplers was significantly lower than the value expected from molecular diffusivities. Supplementary oxidant experiments indicated that depletion of the PTIO oxidant in the Gradko NO_x samplers (currently under development) during exposure is the most likely explanation. Increasing the oxidant loading resulted in proportionally higher nitrite collection from NO, demonstrating that further optimisation of the oxidant formulation may be required to achieve quantitative conversion of NO to NO_2 throughout the exposure period.

This work provided validated traceable measurements to improve the accuracy of three sets of commercially available samplers (Passam NO_2 and NO_x samplers, Gradko NO_2 samplers). It also indicated further test are required to improve the performance of the Gradko NO_x sampler under development. The ability to obtain simultaneous measurements of NO and NO_2 using validated diffusive samplers offers a significant opportunity to expand the spatial coverage of NO_x monitoring at relatively low cost. Such measurements are increasingly important as NO_x emissions continue to decline across many urban areas and regulatory limit values become progressively more stringent. Under these changing conditions, improved understanding of the partitioning between NO and NO_2 is required to support emissions inventory verification, assessment of local interventions and evaluation of air quality models.

Overall, this work demonstrates that diffusive samplers can provide a practical and traceable approach for simultaneous NO and NO_2 monitoring and establishes key performance parameters for NO_x diffusive samplers. The results will support future deployment of NO_x diffusion tube networks and contribute to the ongoing development of European documentary standards for diffusive sampling within CEN/TC 264/WG 11.

https://doi.org/10.5194/egusphere-2026-5280
Preprint. Discussion started: 16 November 2026
© Author(s) 2026. CC BY 4.0 License.

Acknowledgements

We gratefully acknowledge the funding received from the National Measurement System of the UK Department of Science, Innovation and Technology (DSIT), and from the Local Air Quality Management of the UK Department for Environment, Food & Rural Affairs (Defra).

References

Alam, M. S., Crilley, L. R., Lee, J. D., Kramer, L. J., Pfrang, C., Vázquez-Moreno, M., Ródenas, M., Muñoz, A., and Bloss, W. J.: Interference from alkenes in chemiluminescent NO_x measurements, Atmospheric Meas. Tech., 13, 5977–5991, https://doi.org/10.5194/amt-13-5977-2020, 2020.

Brown, R. J. C., Ferracci, V., and Martin, N. A.: Diffusive samplers for ambient air quality monitoring, Anal. Methods, 17, 5074–5077, https://doi.org/10.1039/D5AY90067K, 2025.

BS EN 13528-2:2002: Ambient air quality. Diffusive samplers for the determination of concentrations of gases and vapours. Requirements and test methods - Specific requirements and test methods, 2002.

BS EN 14211:2024: Ambient air. Standard method for the measurement of the concentration of nitrogen dioxide and nitrogen monoxide by chemiluminescence, 2024.

BS EN 16339:2025: Ambient air - Method for the determination of the concentration of nitrogen dioxide by diffusive sampling:, , https://doi.org/10.3403/30472313, 2025.

Butterfield, D., Martin, N. A., Coppin, G., and Fryer, D. E.: Equivalence of UK nitrogen dioxide diffusion tube data to the EU reference method, Atmos. Environ., 262, 118614, https://doi.org/10.1016/j.atmosenv.2021.118614, 2021.

Cape, J. N.: The Use of Passive Diffusion Tubes for Measuring Concentrations of Nitrogen Dioxide in Air, Crit. Rev. Anal. Chem., 39, 289–310, https://doi.org/10.1080/10408340903001375, 2009.

Cliff, S. J., Drysdale, W., Lewis, A. C., Møller, S. J., Helfter, C., Metzger, S., Liddard, R., Nemitz, E., Barlow, J. F., and Lee, J. D.: Evidence of Heating-Dominated Urban NO_x Emissions, Environ. Sci. Technol., 59, 4399–4408, https://doi.org/10.1021/acs.est.4c13276, 2025.

Department for Environment, Food & Rural Affairs: Quality Assurance and Quality Control (QA/QC) Procedures for UK Air Quality Monitoring under the Air Quality Standards Regulations, 2023.

Department for Environment, Food & Rural Affairs: Automatic Urban and Rural Network (AURN), https://uk-air.defra.gov.uk/networks/network-info?view=aurn (last access: 2 November 2025a), 2025.

Department for Environment, Food & Rural Affairs: LAQM Technical Guidance LAQM TG22, 2025b.

Department for Environment, Food & Rural Affairs: NO_2 Diffusion Tube Monitoring Calendar, https://laqm.defra.gov.uk/air-quality/air-quality-assessment/diffusion-tube-monitoring-calendar/, last access: 5 November 2025c, 2025., 2025.

Department for Environment, Food & Rural Affairs: UK Urban NO_2 Network, https://uk-air.defra.gov.uk/networks/network-info?view=UUNN, last access: 18 June 2025d, 2025., 2025.

https://doi.org/10.5194/egusphere-2026-5280
Preprint. Discussion started: 16 November 2026
© Author(s) 2026. CC BY 4.0 License.



Diez, S., Bannan, T. J., Chacón-Mateos, M., Edwards, P. M., Ferracci, V., Kılıç, D., Lewis, A. C., Malings, C., Martin, N. A., Popoola, O., Rosales, C., Schmitz, S., Schneider, P., and von Schneidemesser, E.: A framework for advancing independent air quality sensor measurements via transparent data generating process classification, Npj Clim. Atmospheric Sci., 8, 285, https://doi.org/10.1038/s41612-025-01161-2, 2025.

EU Directive 2008/50/EC: Directive 2008/50/EC of the European Parliament and of the Council of 21 May 2008 on ambient air quality and cleaner air for Europe, 2008.

EU Directive 2024/2881: Directive (EU) 2024/2881 of the European Parliament and of the Council of 23 October 2024 on ambient air quality and cleaner air for Europe, 2024.

Ferracci, V., Brown, A. S., Harris, P. M., and Brown, R. J. C.: An investigation of the matrix sensitivity of refinery gas analysis using gas chromatography with flame ionisation detection, J. Chromatogr. A, 1383, https://doi.org/10.1016/j.chroma.2015.01.030, 2015.

Hafkenscheid, T., Fromage-Mariette, A., Goelen, E., Hangartner, M., and Pfeffer, U.: Review of the application of diffusive samplers in the European Union for the monitoring of nitrogen dioxide in ambinet air, Office for Official Publications of the European Communities, Luxembourg, 2009.

Hayward, I., Martin, N. A., Ferracci, V., Kazemimanesh, M., and Kumar, P.: Low-Cost Air Quality Sensors: Biases, Corrections and Challenges in Their Comparability, Atmosphere, 15, 1523, https://doi.org/10.3390/atmos15121523, 2024.

Heal, M. R. and Cape, J. N.: A numerical evaluation of chemical interferences in the measurement of ambient nitrogen dioxide by passive diffusion samplers, Atmos. Environ., 31, 1911–1923, https://doi.org/10.1016/S1352-2310(97)00025-3, 1997.

Heal, M. R., O'Donoghue, M. A., and Cape, J. N.: Overestimation of urban nitrogen dioxide by passive diffusion tubes: a comparative exposure and model study, Atmos. Environ., 33, 513–524, https://doi.org/10.1016/S1352-2310(98)00290-8, 1999.

Heal, M. R., Laxen, D. P. H., and Marner, B. B.: Biases in the Measurement of Ambient Nitrogen Dioxide (NO_2) by Palmes Passive Diffusion Tube: A Review of Current Understanding, Atmosphere, 10, 357, https://doi.org/10.3390/atmos10070357, 2019.

Kebabian, P. L., Wood, E. C., Herndon, S. C., and Freedman, A.: A Practical Alternative to Chemiluminescence-Based Detection of Nitrogen Dioxide: Cavity Attenuated Phase Shift Spectroscopy, Environ. Sci. Technol., 42, 6040–6045, https://doi.org/10.1021/es703204j, 2008.

Laitinen, J., Liesivuori, J., Linnainmaa, M., and Kalliokoski, P.: Evaluation of monitoring methods for nitrogen oxides, Ann. Occup. Hyg., 37, 307–314, https://doi.org/10.1093/annhyg/37.3.307, 1993.

Martin, N. A., Marlow, D. J., Henderson, M. H., Goody, B. A., and Quincey, P. G.: Studies using the sorbent Carbopack X for measuring environmental benzene with Perkin–Elmer-type pumped and diffusive samplers, Atmos. Environ., 37, 871–879, https://doi.org/10.1016/S1352-2310(02)01000-2, 2003.

Martin, N. A., Duckworth, P., Henderson, M. H., Swann, N. R. W., Granshaw, S. T., Lipscombe, R. P., and Goody, B. A.: Measurements of environmental 1,3-butadiene with pumped and diffusive samplers using the sorbent Carbopack X, Atmos. Environ., 39, 1069–1077, https://doi.org/10.1016/j.atmosenv.2004.09.078, 2005.

https://doi.org/10.5194/egusphere-2026-5280
Preprint. Discussion started: 16 November 2026
© Author(s) 2026. CC BY 4.0 License.

Martin, N. A., Helmore, J. J., White, S., Barker Snook, I. L., Parish, A., and Gates, L. S.: Measurement of nitrogen dioxide diffusive sampling rates for Palmes diffusion tubes using a controlled atmosphere test facility (CATFAC), Atmos. Environ., 94, 529–537, https://doi.org/10.1016/j.atmosenv.2014.05.064, 2014.

Martin, N. A., Ferracci, V., Cassidy, N., Hook, J., Battersby, R. M., Meane, E. A. D., Tang, Y. S., Stephens, A. C. m., Leeson, S. R., Jones, M. R., Braban, C. F., Gates, L., Hangartner, M., Stoll, J., Sacco, P., Pagani, D., Hoffnagle, J. A., and Seitler, E.: Validation of ammonia diffusive and pumped samplers in a controlled atmosphere test facility using traceable Primary Standard Gas Mixtures, Atmos. Environ., 199, 453–462, https://doi.org/S1352231018308185, 2019.

Massman, W. J.: A review of the molecular diffusivities of H2O, CO2, CH4, CO, O3, SO2, NH3, N2O, NO, and NO2 in air, O2 and N2 near STP, Atmos. Environ., 32, 1111–1127, https://doi.org/10.1016/S1352-2310(97)00391-9, 1998.

Mead, M. I., Popoola, O. A. M., Stewart, G. B., Landshoff, P., Calleja, M., Hayes, M., Baldovi, J. J., McLeod, M. W., Hodgson, T. F., Dicks, J., Lewis, A., Cohen, J., Baron, R., Saffell, J. R., and Jones, R. L.: The use of electrochemical sensors for monitoring urban air quality in low-cost, high-density networks, Atmos. Environ., 70, 186–203, https://doi.org/10.1016/j.atmosenv.2012.11.060, 2013.

Medland, D., Garcia, G., Gardiner, T., Martin, N. A., Ferracci, V., Wilkins, A., Fryer, D., Holmes, T., Edwards, P., Diez, S., and Butterfield, D.: Comparison of NO_2 diffusion tube measurement methods and related uncertainties, Atmos. Environ., 352, 121219, https://doi.org/10.1016/j.atmosenv.2025.121219, 2025.

Palmes, E. D., Gunnison, A. F., DiMattio, J., and Tomczyk, C.: Personal sampler for nitrogen dioxide, Am. Ind. Hyg. Assoc. J., 37, 570–577, https://doi.org/10.1080/0002889768507522, 1976.

Passam AG: Diffusive Sampler for Total Nitrogen NO_x, 2020.

Popoola, O. A. M., Carruthers, D., Lad, C., Bright, V. B., Mead, M. I., Stettler, M. E. J., Saffell, J. R., and Jones, R. L.: Use of networks of low cost air quality sensors to quantify air quality in urban settings, Atmos. Environ., 194, 58–70, https://doi.org/10.1016/j.atmosenv.2018.09.030, 2018.

Sánchez Jiménez, A., Heal, M. R., and Beverland, I. J.: Intercomparison study of NO_x passive diffusion tubes with chemiluminescence analysers and evaluation of bias factors, Atmos. Environ., 45, 3062–3068, https://doi.org/10.1016/j.atmosenv.2011.03.011, 2011.

Smith, I. M.: Software for determining polynomial calibration functions by generalised least squares: user manual., MS11, https://eprintspublications.npl.co.uk/4830/ (last access: 14 May 2025), 2010.

UK Environment Act 2021: UK Environment Act, 2021.

Vardoulakis, S., Lumbreras, J., and Solazzo, E.: Comparative evaluation of nitrogen oxides and ozone passive diffusion tubes for exposure studies, Atmos. Environ., 43, 2509–2517, https://doi.org/10.1016/j.atmosenv.2009.02.048, 2009.

Vestreng, V., Ntziachristos, L., Semb, A., Reis, S., Isaksen, I. S. A., and Tarrasón, L.: Evolution of NO_x emissions in Europe with focus on road transport control measures, Atmospheric Chem. Phys., 9, 1503–1520, https://doi.org/10.5194/acp-9-1503-2009, 2009.

Villena, G., Bejan, I., Kurtenbach, R., Wiesen, P., and Kleffmann, J.: Interferences of commercial NO_2 instruments in the urban atmosphere and in a smog chamber, Atmospheric Meas. Tech., 5, 149–159, https://doi.org/10.5194/amt-5-149-2012, 2012.

https://doi.org/10.5194/egusphere-2026-5280
Preprint. Discussion started: 16 November 2026
© Author(s) 2026. CC BY 4.0 License.



World Health Organization: Economic cost of the health impact of air pollution in Europe: clean air, health and wealth, WHO/EURO:2015-4102-43861-61759, https://www.who.int/europe/publications/i/item/WHO-EURO-2015-4102-43861-61759 (last access: 14 May 2025), 2015.